[4] E. G. Cristal and G. L. Matthaei, "A technique for the design of multiplexers having contiguous channels," *IEEE Trans. Microwave Theory Tech.*, vol. MTT-12, pp. 88–93 (see p. 89), Jan. 1964.
[5] R. E. DeBrecht, "Coplanar balun circuits for GaAs FET high-power push-pull amplifiers," in *IEEE-GMTT Int. Microwave Symposium Digest* (Univ. of Colorado, June 1973), pp. 309–311.
[6] R. Sato and E. G. Cristal, "Simplified analysis of coupled transmission line networks," *IEEE Trans. Microwave Theory Tech.*, vol. MTT-18, pp. 122–131, Mar. 1970.
[7] J. A. Weiss and T. G. Bryant, "Even and odd mode characteristic impedance for coupled microstrip," *Microwave Engineer's Handbook*, vol. 1. Dedham, Massachusetts: Artech House, 1971, pp. 132–133.

# A Nonlinear Analysis of Schottky-Barrier Diode Upconverters

MASAMI AKAIKE, MEMBER, IEEE, AND KAZUHITO OHNISHI

*Abstract*—**A nonlinear computer analysis of Schottky-barrier diode upconverters by means of obtaining the steady-state solutions of differential equations characterized by the diode and connected circuits is shown. Both the nonlinearities of barrier resistance and capacitance are taken into consideration. The waveforms of the voltage and current at the diode, impedance, and input–output power relationships are computed for 120-GHz upconverters.**

## I. Introduction

FREQUENCY upconverters have been widely used in transmitters of the microwave and millimeter-wave transmission systems. There are two kinds of diodes used: Schottky-barrier diodes and p-n-junction varactor diodes. In varactor diode upconverters, since a sufficient dc bias voltage is applied reversely to the diode and no conduction current flows during operation, frequency conversion is performed through only the nonlinearity of the junction capacitance. In Schottky-barrier diode upconverters, however, the forward conduction current flows across the barrier during a certain period of time whereas the diode is reversely biased, and both the nonlinearities of barrier resistance and junction capacitance contribute to frequency conversion.

For designing the upconverter circuit and diode to be used, it is necessary to know their characteristics, such as the impedances, input–output power relationship, and voltage and current waveforms at the diode. For varactor upconverters, there have been excellent theoretical papers already reported,[1] and various fundamental characteristics have been made clear. As for Schottky-barrier diode upconverters, however, since the frequency conversion mechanism is related to two nonlinearities, and the current- or voltage-excitation model commonly assumed in varactor upconverters is not realistic, the treatment is more complex, and perhaps the analytical calculation is impossible.

According to the past experience on millimeter-wave upconverters, Schottky-barrier diodes exhibited better characteristics with respect to ease in circuit adjustment and suppression of unwanted spurious oscillations [1]. In the guided millimeter-wave transmission system in Japan, W-40G system, Schottky-barrier diode upconverters were preferred for that reason [2]. Although Schottky-barrier diode upconverters are believed to be very important components in practical communication systems in the microwave region and above, there have been no theoretical papers dealing with their characteristics in detail.

It is the purpose of this paper to present a theoretical investigation of Schottky-barrier diode upconverters by means of computer-aided numerical analysis. There are two approaches of analysis possible: 1) the time-domain approach in which differential equations of voltage and current, with respect to time are built, and their steady-state solutions are obtained, and 2) the frequency-domain approach in which the voltage and current components of specific frequencies are first assumed, simultaneous equations with respect to these components are made utilizing the voltage–current relationship of the diode, and then they are solved.

The time-domain approach is used in the present paper. Although this method of analysis can be used for any frequency, the present computation is performed at 120 GHz. In the analysis the following points are assumed.

1) An unencapsulated diode is directly mounted in the waveguide, i.e., the diode case capacitance is not considered. Furthermore, the equivalent circuit of the diode is somewhat simplified. The parameters of the diode used in the computation are determined by small-signal measurement. A detailed discussion is given in Section II.

Manuscript received May 17, 1977; revised July 16, 1977.
The authors are with the Yokosuka Electrical Communication Laboratory, Nippon Telegraph and Telephone Public Corporation, Yokosuka-shi, Kanagawa-ken, 238-03 Japan.

[1] There have already been published good textbooks on varactor diodes and their applications, such as H. A. Watson, *Microwave Semiconductor Devices and Their Circuit Applications*, New York: McGraw-Hill, 1969, and M. Miyagawa, *Varactor Diodes and Their Applications*, Tokyo, Japan: Industrial Daily News, Ltd., 1969. Original papers are found in these textbooks.

2) Three external circuits are connected to the diode, and the current components of all frequencies flowing into and generated from the diode flow in either of these three circuits. The impedance of each external circuit takes the same value for all frequencies. This is approximately valid when the local-oscillator (LO) frequency is much higher than the intermediate frequency (IF), and the output power levels of harmonics of LO frequency and IF are very low compared to these two input power levels. We will discuss on this point later in Sections III and IV in more detail.

3) The ratio of the LO frequency to the IF is equal to an integer $n$. With this assumption, we can easily obtain the steady-state solutions of voltage and current waveforms.

## II. Equivalent Circuit and Parameters of a Schottky-Barrier Diode

Since the characterization of the diode to be used is our first concern, the equivalent circuit of a Schottky-barrier diode and its parameters are discussed here. The actual equivalent circuit of an unencapsulated diode, directly mounted in a waveguide, is rather complex, since the parasitic capacitance between the whisker and the waveguide wall is added in parallel to the junction and series resistance (Fig. 1(a)). The major part of the series resistance $R_s$ is the spreading resistance inside the semiconductor epitaxial layer. Although the parasitic parallel capacitances are connected in an intricate manner in terms of equivalent circuit depending upon their distances from the junction, we divide them, for simplicity, collectively into two lumps $C_{p1}$ and $C_{p2}$. $C_{p1}$ represents the capacitance which exists very near the junction, and $C_{p2}$ the total parasitic capacitance which exists between the whisker and the waveguide wall, more than several times the junction diameter away from the junction. Since the spreading resistance is mainly determined by the region within several times the junction diameter, $C_{p2}$ is approximately considered to be added outside $R_s$. In practical cases, the junction capacitance being fairly large compared to $C_{p2}$,[2] the equivalent circuit of Fig. 1(a) is approximately simplified as shown in Fig. 1(b). It should be noted that $C_{Je}$ includes $C_{p1}$ and $C_{p2}$, as well as the real junction capacitance $C_J$, and $R_{se}$ is a function of $C_{p1}$, $C_{p2}$, and $C_J$. We use this simplified equivalent circuit of Fig. 1(b) in the computation. Furthermore, we assume that $C_{Je}$ is expressed as the form[3]

$$C_{Je} = C_0(1 - V_B/\phi)^{-\gamma} \tag{1}$$

where $\phi$ and $V_B$ are the diffusion voltage and the voltage across the barrier, respectively, and we call $C_0$ and $\gamma$ the junction capacitance at zero bias and the slope factor of capacitance, respectively.

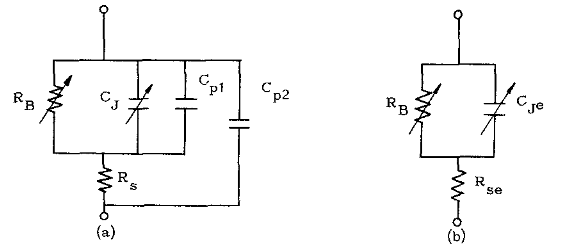

$R_B$ : Barrier resistance

$C_J$ : Junction capacitance

$C_{p1}$, $C_{p2}$ : Parasitic capacitances

$R_s$ : Series resistance

For $C_J^2 \gg C_{p2}^2$

$C_{Je} \simeq C_J + C_{p1} + C_{p2}$

$R_{se} \simeq R_s \cdot \dfrac{(C_J + C_{p1})^2}{(C_J + C_{p1} + C_{p2})^2}$

Fig. 1. Equivalent circuit of a Schottky-barrier diode directly mounted in a waveguide. (a) The parasitic capacitance between the whisker and the waveguide wall is divided into two lumps $C_{p1}$ and $C_{p2}$. (b) When $C_J$ is fairly large compared to $C_{p2}$, the equivalent circuit can be simplified. We assume the form $C_{Je} = C_0(1 - V_B/\phi)$.

TABLE I
Diode Parameters Used in the Upconverters

| | |
|---|---|
| $I_s$ | Saturation current, $1.4 \times 10^{-14}$ A |
| $\eta$ | Slope factor of current, 1.1 |
| $R_{se}$ | Series resistance, 17 Ω |
| $C_{Je}$ | Junction capacitance, $C_{Je} = C_0\,(1 - V_B/\phi)^{-\gamma}$ |
| $C_0$ | Junction capacitance at zero-bias, 0.03 pF |
| Q | Quality factor of diode, $Q = 1/(2\pi f_{LO} C_0 R_{se})$ |
| $\gamma$ | Slope factor of capacitance, 0.3 |
| $\phi$ | Diffusion voltage, 0.85 V |
| e/kT | = 40 [1/V] at room temperature |

*Note:* $I_s$ and $\eta$ were measured at dc. $R_{se}$, $C_{Je}$, and $C_0$ were measured at 120 GHz and include parasitic capacitances.

As is well known, the voltage–current relationship of a Schottky-barrier diode is expressed as[4]

$$\begin{aligned} I_T &= I_s[\exp\,(eV_B/\eta kT) - 1] + C_0(1 - V_B/\phi)^{-\gamma}\, dV_B/dt \\ V_T &= R_{se} I_T + V_B \end{aligned} \tag{2}$$

where $V_T$ is the voltage across the diode terminals, $I_T$ is the sum of the conduction and displacement currents, $I_s$ is the saturation current, $\eta$ is the slope factor of current, and $e/kT \cong 40$ at room temperature. $I_s$ and $\eta$ are determined from the $V$–$I$ curve measured at dc and its plots on a linear–logarithmic scale [5]. It is commonly assumed that these two quantities do not change with frequency. However, $R_{se}$, $C_0$, and $\gamma$ should be determined from RF measurement, since the equivalent circuit of Fig. 1(b) is an approximate form. The authors measured $R_{se}$, $C_0$, and $\gamma$ with n-type GaAs Schottky-barrier diodes with different diameters and listed the average values for 5-$\mu$m-diameter diodes[5] in Table I. We use these values in the computation.

[2] According to a theoretical consideration, $C_{p1} \cong C_{p2} \cong 0.004$ pF for the usual whisker dimension [3], whereas the junction capacitance at zero bias measured by the authors (the form of Fig. 1(b) assumed) is 0.02–0.03 and 0.06–0.08 pF for 5-$\mu$m and 10-$\mu$m diameter n-GaAs Schottky-barrier diodes, respectively.

[3] In a strict sense, the quantity $\gamma$ is not constant for any value of $V_B$ and it deviates from 0.5 of the ideal one-dimensional case, because 1) $C_{Je}$ contains $C_{p1}$ and $C_{p2}$, and 2) the depletion layer extends itself with increasing $V_B$ in the direction of diameter in a planar-type diode [4]. However, we approximated it as constant, and determined it from measurement.

[4] The conduction current is assumed to be not affected by parasitic capacitances.

[5] Although the impurity concentration and thickness of the semiconductor epitaxial layer were slightly different for different diodes, they were, respectively, $2 \times 10^{23}/\mathrm{m}^3$ and 1 $\mu$m on the average. The measurement was made with the diode mounted in a waveguide wafer-type diode holder. Therefore, $R_{se}$ includes circuit losses near the junction.

In the last part of Section V, however, $Q$ (the quality factor of diode, $= 1/\omega C_0 R_{se}$) and $\gamma$ are varied in order to examine a more extensive relationship between upconverter characteristics and diode parameters.

Although the series resistance $R_{se}$ is mainly determined by the spreading resistance in the semiconductor epitaxial layer, and the depletion layer is a function of $V_B$, let us assume that the equivalent circuit parameters measured at small-signal levels are valid for large RF and IF excitations.

## III. Circuit Description

The upconverter circuit discussed in the present paper is shown in Fig. 2. Three circuits are connected to a Schottky-barrier diode[6]: a millimeter-wave circuit (the millimeter-wave circuit represents both the LO circuit and output circuit), an IF circuit, and a dc circuit. Each circuit has an excitation or a signal source: an LO whose frequency is $f_{\mathrm{LO}}$, an IF source whose frequency is $f_{\mathrm{IF}}$, and a dc bias source. These three circuits are separated by three ideal filters, each of which presents short-circuits for particular frequencies and open-circuits at other frequencies. Since the diode is capacitive, inductances are connected in the millimeter-wave and IF circuits to match their impedances to the diode. The inductance in the dc circuit is a choke inductor.

From voltage–current relationships of the diode, and the connected circuits, one obtains a set of differential equations with respect to IF phase angle $\theta$ ($\theta = \Omega t$, $\Omega = 2\pi f_{\mathrm{IF}}$) as follows:

$$dI_{\mathrm{MM}}/d\theta = [E_{\mathrm{MM}} \sin n\theta - R_{\mathrm{MM}} I_{\mathrm{MM}} - R_{se} I_T - V_B - V_{\mathrm{FMM}}]/(\Omega L_{\mathrm{MM}}) \tag{3}$$

$$dI_{\mathrm{IF}}/d\theta = [E_{\mathrm{IF}} \sin(\theta + p) - R_{\mathrm{IF}} I_{\mathrm{IF}} - R_{se} I_T - V_B - V_{\mathrm{FIF}}]/(\Omega L_{\mathrm{IF}}) \tag{4}$$

$$dI_{\mathrm{DC}}/d\theta = [E_{\mathrm{DC}} - R_{\mathrm{DC}} I_{\mathrm{DC}} - R_{se} I_T - V_B - V_{\mathrm{FDC}}]/(\Omega L_{\mathrm{DC}}) \tag{5}$$

$$dV_B/d\theta = [I_{\mathrm{MM}} + I_{\mathrm{IF}} + I_{\mathrm{DC}} - I_s \cdot \{\exp(eV_B/\eta kT) - 1\}]/(\Omega C_{Je}) \tag{6}$$

where $n$ is an integer and shows the ratio of $f_{\mathrm{LO}}$ to $f_{\mathrm{IF}}$, $I_T = I_{\mathrm{MM}} + I_{\mathrm{IF}} + I_{\mathrm{DC}}$, and $p$ is the IF-phase angle. In these equations, the first three equations correspond to the three external circuits, and the last equation to the diode. The unknown variables to be solved are $I_{\mathrm{MM}}$, $I_{\mathrm{IF}}$, $I_{\mathrm{DC}}$, and $V_B$.

Each resistance and inductance is assumed to take the same value for all frequencies. This assumption is in appearance not appropriate from two viewpoints: 1) first, the characteristic impedance of a rectangular waveguide is a function of frequency, and 2) second, the impedances for higher order modes are likely to be different from the fundamental-mode impedance. However, when the IF is very low compared to the LO frequency (this is a very common case) the difference in characteristic impedance with frequency can be neglected for sidebands near the LO frequency. And since the level of the sideband decreases rapidly as its frequency goes away from the LO frequency, different termination for these sidebands has less significant effect on the signal output power. The effect of $2f_{\mathrm{IF}}$ on the signal output power is discussed in the following section.

[6] In a practical diode, $R_s$ is a function of frequency, since it contains the circuit loss, and the skin depth is a function of frequency. However, in this analysis, $R_s$ is assumed constant for different frequencies.

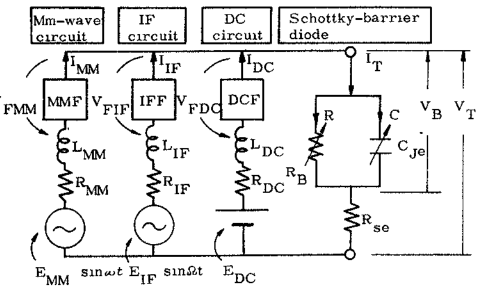


$$I_R = I_s[\exp(eV_B/\eta kT) - 1],\ I_C = C_{Je}\, dV_B/dt,\ C_{Je} = C_o(1 - V_B/\phi)^{-\gamma}$$

$$I_T = I_R + I_C = I_{\mathrm{MM}} + I_{\mathrm{IF}} + I_{\mathrm{DC}}$$

$$\omega = 2\pi f_{\mathrm{LO}},\ \Omega = 2\pi f_{\mathrm{IF}},\ \omega = n\Omega$$

$$V_T = I_T R_{se} + V_B$$

Fig. 2. Circuit construction of the upconverter. Three circuits (a millimeter-wave, an IF, and a dc circuit) are connected to a Schottky-barrier diode.

In the dc circuit we allow only dc current to flow. In the IF circuit we allow the IF current components from $f_{\mathrm{IF}}$ to $mf_{\mathrm{IF}}$. In the millimeter-wave circuit we allow the current components higher than $mf_{\mathrm{IF}}$. Then the voltage drops across the filters $V_{\mathrm{FMM}}$, $V_{\mathrm{FIF}}$, and $V_{\mathrm{FDC}}$, are expressed as

$$V_{\mathrm{FMM}} = -\sum_{|i| \le m} V_{Ti} e^{ji\Omega t} \qquad V_{\mathrm{FIF}} = -\sum_{|i| \ge (m+1), =0} V_{Ti} e^{ji\Omega t}$$

$$V_{\mathrm{FDC}} = -\sum_{i \ne 0} V_{Ti} e^{ji\Omega t} \tag{7}$$

where $V_{Ti}$ is the $i$th Fourier component of $V_T[= R_{se}(I_{\mathrm{MM}} + I_{\mathrm{IF}} + I_{\mathrm{DC}}) + V_B]$. $mf_{\mathrm{IF}}$ is chosen to be near the cutoff frequency of the waveguide which is used for the millimeter-wave circuit.

## IV. Numerical Computation

By computing the steady-state solutions of (3)–(6), and by their Fourier components with respect to $f_{\mathrm{LO}}$, $f_{\mathrm{IF}}$, and $f_{\mathrm{OUT}}$, one can determine the voltage and current waveforms at the diode, impedances, and input–output power relationship of the upconverter. An upper-sideband upconverter is considered here. Therefore, the output frequency $f_{\mathrm{OUT}}$ is the sum of $f_{\mathrm{LO}}$ and $f_{\mathrm{IF}}$.

The computation process is shown in more detail in Fig. 3 and below.

### A. Voltage Drops Across the Filters ($V_{\mathrm{FMM}}$, $V_{\mathrm{FIF}}$, $V_{\mathrm{FDC}}$)

First we assume the constants in (3)–(6) at appropriate values: the diode parameters listed in Table I, source voltages ($E_{\mathrm{MM}}$, $E_{\mathrm{IF}}$, and $E_{\mathrm{DC}}$), resistances and inductances of the three external circuits. Then we solve the differential equations over one period of IF and obtain steady-state solutions of four variables by means of the Runge–Kutta–Gill method. From their Fourier components (obtained by

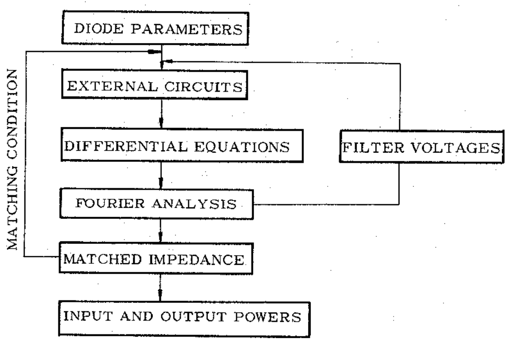


Fig. 3. A detailed computation process.

the fast Fourier transform) and (7), more accurate voltage drops of the filters are given. Correct values are obtained by iterating this process.

### B. Matched Impedances

In order to utilize the LO and IF powers effectively, the impedances of the external circuits are necessary to be matched to the diode. Since the input impedances of the diode looked at the IF and LO frequency are $V_{T1}/I_{T1}$ and $V_{Tn}/I_{Tn}$, respectively, the resistances and inductances are varied so as to satisfy the following equations:

$$R_{MM} + j\omega L_{MM} = [V_{Tn}/I_{Tn}]^*$$
$$R_{IF} + j\Omega L_{IF} = [V_{T1}/I_{T1}]^* \tag{8}$$

where $I_{Ti}$ is the $i$th Fourier component of $I_T$, and the asterisk denotes the complex conjugate.

### C. Computation of Characteristics

By iterating processes (A) and (B), we can obtain various upconverter characteristics, such as the voltage and current waveforms, matched impedances, and input–output power relationship with a sufficient accuracy. The available powers of the LO and IF source, $P_{LO}$ and $P_{IF}$, their delivered powers to the diode, $P_{LO\,IN}$ and $P_{IF\,IN}$, and output power $P_{OUT}$ are represented by

$$P_{LO} = |E_{MM}|^2/8R_{MM} \qquad P_{IF} = |E_{IF}|^2/8R_{IF}$$
$$P_{LO\,IN} = 2\ \mathrm{Re}\ [V_{Tn}I_{Tn}^*] \qquad P_{IF\,IN} = 2\ \mathrm{Re}\ [V_{T1}I_{T1}^*]$$
$$P_{OUT} = -2\ \mathrm{Re}\ [V_{Tn+1}I_{Tn+1}^*]. \tag{9}$$

When the LO and IF impedances are sufficiently matched to the diode, $P_{LO}$ and $P_{IF}$ are very close to $P_{LO\,IN}$ and $P_{IF\,IN}$, respectively.

## V. Computed Results

Let us compute upconverter characteristics for $f_{LO} = 110$ GHz, $f_{IF} = 11$ GHz, and $f_{OUT} = 121$ GHz. In the 120-GHz range, the R-1200 rectangular waveguide (frequency: 90–140 GHz; inside dimension: $2.032 \times 1.016$ mm$^2$) is commonly used. Since the cutoff frequency of this waveguide is 73.7 GHz, $m$ in (7) is set at seven in the computation. The diode parameters used are listed in Table I. Let $R_{DC} = 300\ \Omega$, $E_{DC} = 0$ V (the diode is self-biased) and $p$ in (4) be zero.

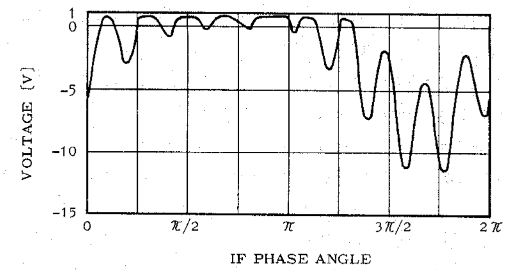


Fig. 4. Waveform of $V_B$ as a function of IF phase angle for $P_{LO} = P_{IF} =$ 12.5 dBm.

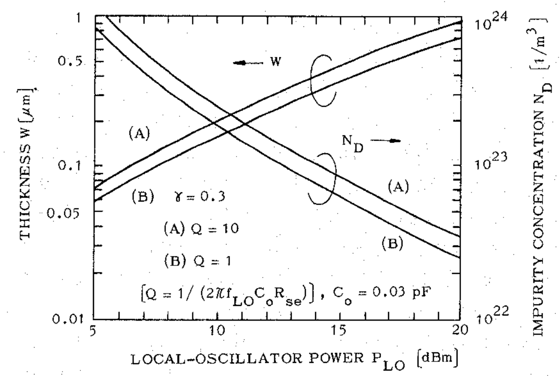


Fig. 5. The impurity concentration and thickness of the diode epitaxial layer which give just punchthrough when the reverse voltage reaches its maximum. $P_{LO} = P_{IF}$. Input power to the diode is $P_{LO} + P_{IF}$.

Fig. 4 shows the waveform of the voltage across the barrier ($V_B$) as a function of IF phase angle. It shows that the voltage waveform is far from being sinusoidal. The reverse waveform is important, because from the maximum reverse voltage, we can determine a necessary breakdown voltage of the diode. Breakdown voltage is related to impurity concentration and thickness of the semiconductor epitaxial layer [4]. Therefore, we can specify impurity concentration and thickness of the diode epitaxial layer from the analysis. When the maximum reverse voltage exceeds the breakdown voltage of the diode, the avalanche breakdown current flows, and the junction is probably thermally broken. If the breakdown voltage is much higher than the maximum reverse voltage, on the other hand, unswept region of the epitaxial layer provides excess series resistance which degrades the diode $Q$. The impurity concentration and thickness, which give just punchthrough when the reverse voltage reaches its maximum, are shown in Fig. 5. This offers one measure when we design diode material constants.

The current waveform is shown in Fig. 6. The solid line is the total current, and the dotted line is the conduction current through the barrier resistance. The conduction current flows during about half a cycle of IF, and the displacement current dominates in the other half cycle. This means that the nonlinearity of capacitance, as well as the nonlinearity of resistance, also contributes to frequency conversion efficiency in Schottky-barrier diode upconverters.

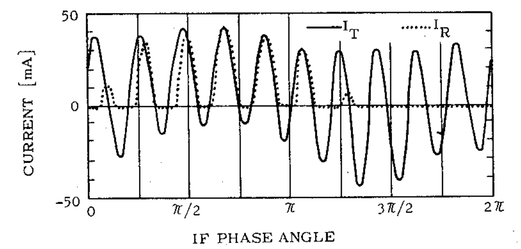


Fig. 6. Waveform of current as a function of IF phase angle for $P_{LO} = P_{IF} = 12.5$ dBm. ———: total current; - - - - -: conduction current through the barrier resistance.

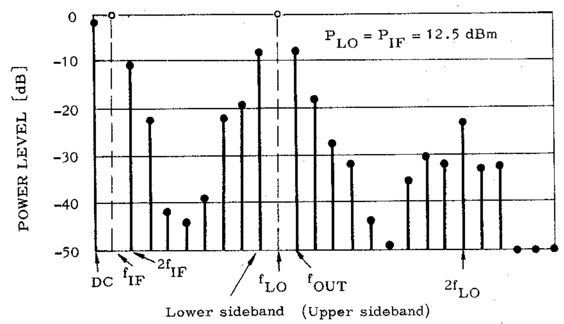


Fig. 7. Power spectra. Broken lines show input powers ($P_{IF}$ and $P_{LO}$) and solid lines show generated powers from the diode. $P_{LO} = P_{IF} = 12.5$ dBm.

The power spectra are shown in Fig. 7. The broken lines show the input powers ($P_{LO\,IN}$ and $P_{IF\,IN}$), and the solid lines show generated powers from the diode. The lower sideband has approximately the same power level as the upper sideband. These power spectra offer important information in designing the filters for suppressing spurious interferences, and in estimating the reliability of diodes in practical transmission systems.

It has been assumed that the impedance in each external circuit takes the same value for all frequencies. The effect of different termination for harmonic frequencies is discussed here. Let us assume that the input–output power relationship is linear. Fig. 7 tells us that the signal output power ($f_{LO} + f_{IF}$ component) generated by the mixing of $2f_{IF}$ and $f_{LO} - f_{IF}$ is about 30 dB below the LO (or IF) power level, and by $2f_{LO}$ and $f_{LO} - f_{IF}$ is more than 40 dB below. Consequently, even if the terminations with respect to $2f_{LO}$ and $f_{LO}$, and to $2f_{IF}$ and $f_{IF}$ are different, i.e., even if the second-harmonic impedance is quite different from the fundamental mode impedance, the output power is little affected (within a few percent) by it.

Fig. 8 shows input impedances $Z_{DMM}$ and $Z_{DIF}$ of the diode looked at LO frequency and IF. Although the resistive components of $Z_{DMM}$ and $Z_{DIF}$ increase gradually with increasing $P_{IF}$, they are expressed as

$$\text{Re}\,[Z_{DMM}] \cong R_s(1 + \xi Q)$$
$$\text{Re}\,[Z_{DIF}] \cong R_s(1 + n\xi Q), \qquad \xi \cong 0.6 - 0.7 \qquad (10)$$

where $Q$ is the quality factor of the diode and $n = f_{LO}/f_{IF}$. Above equations are useful in designing practical circuits.

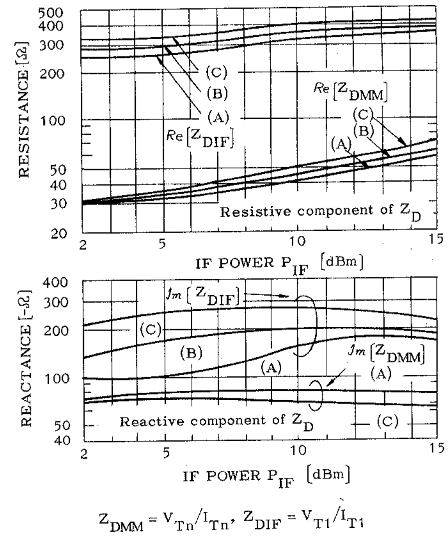


Fig. 8. Diode impedances looked at IF and local-oscillator frequency as a function of IF power $P_{IF}$. $P_{LO}$ is 14 dBm for (A), 11 dBm for (B), and 8 dBm for (C).

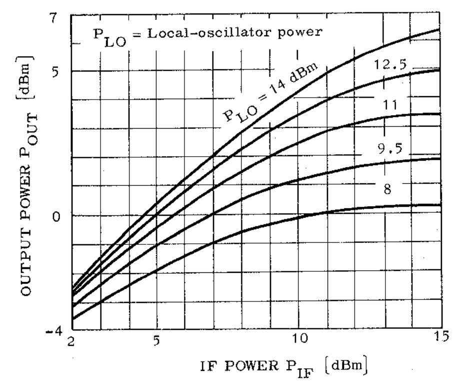


Fig. 9. Input and output power relationship of the upconverter.

The input–output power relationship is shown in Fig. 9 for various LO powers $P_{LO}$. When the IF power is very low, the output power increases linearly with IF power. And then a saturation effect occurs when the IF power becomes comparable to the LO power. The authors have built an experimental upconverter at 120 GHz. The experimental result showed a good agreement with the theoretical analysis [6].

So far, we have shown computed results for fixed diode parameters. In order to get a more extensive view, we examine how the diode parameters affect the power conversion efficiency. Efficiency is often represented by conversion loss, which is the ratio of $P_{IF}$ (or $P_{LO}$) to $P_{OUT}$. The parameters which mainly determine the quality of the diode are the diode $Q$, slope factor of capacitance $\gamma$, and slope factor of current $\eta$. Since $\eta$ is very close to unity for usual Schottky-barrier diodes, the conversion loss for various $Q$ and $\gamma$ are computed here. For simplicity, let $P_{LO} = P_{IF}$. Fig. 10 shows the conversion loss versus $Q$ for different excitation levels. When $Q$ is small, the conversion loss increases rapidly as $Q$ decreases. As $Q$ is inversely proportional to frequency,

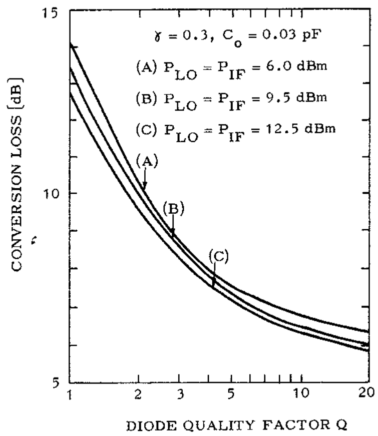


Fig. 10. Conversion loss versus diode quality factor $Q$ for different excitation levels.

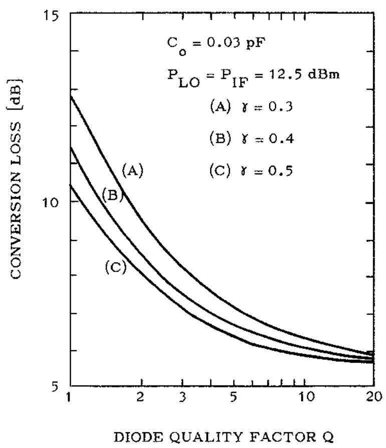


Fig. 11. Conversion loss versus diode quality factor $Q$ for different $\gamma$.

one can regard Fig. 10 as the conversion loss as a function of frequency. Fig. 11 is the conversion loss versus $Q$ for different $\gamma$. For diodes with lower $Q$, the conversion loss is more affected by $\gamma$.

## VI. Conclusion

A computer-aided time-domain nonlinear analysis of Schottky-barrier diode upconverters has been shown. The numerical computation has been performed in the 120-GHz range. By the theoretical analysis, the fundamental characteristics of upconverters, such as the voltage and current waveforms at the diode, matched impedances, and input–output power relationship, have been predicted.

Since the analysis basically utilizes the steady-state solutions of differential equations characterized by the diode and its external circuits, this concept is readily applicable to other large-signal Schottky-barrier diode devices such as frequency multipliers and modulators.


## Acknowledgment

The authors wish to express their thanks to Dr. K. Miyauchi, Dr. S. Shimada, Dr. H. Kimura, Dr. S. Seki, and Dr. M. Fujimoto for their encouragement and guidance, and to Dr. N. Kanmuri and K. Yamamoto for their valuable discussions.


## References


[1] N. Kanmuri, "A study on millimeter-wave frequency converters," doctoral dissertation, Waseda University, Tokyo, Japan, 1977.

[2] M. Akaike, N. Kanmuri, H. Kato, and K. Hiyama, "Millimeter-wave solid-state circuits," *Rev. Elec. Commun. Lab.*, vol. 23, no. 7–8, pp. 904–918, July/Aug. 1975.

[3] Y. Ishii, S. Ogawa, T. Yagasaki, and H. Niiyama, "Millimeter-wave GaAs bond diodes ECL-2170, -2171," *Elec. Commun. Lab. Tech. J.*, vol. 18, no. 7, pp. 1669–1705, 1969.

[4] S. M. Sze, *Physics of Semiconductor Devices.* New York: Wiley, 1969.

[5] H. C. Torrey and C. A. Whitmer, *Crystal Rectifiers.* New York: McGraw-Hill, 1948.

[6] M. Akaike, "Schottky-barrier diode converters in the short millimeter wavelengths region," in *1977 IEEE MTT-S Int. Microwave Symp., Dig. Tech. Papers.*